HHS Public Access

Author manuscript

J Biomech. Author manuscript; available in PMC 2022 August 26.

Published in final edited form as:

J Biomech. 2021 August 26; 125: 110580. doi:10.1016/j.jbiomech.2021.110580.

Effects of chondrogenic priming duration on mechanoregulation of engineered cartilage

Anna M. McDermott[1,2,*], **Emily A Eastburn**[1,3,*], **Daniel J. Kelly**[4,†], **Joel D. Boerckel**[1,2,3,†]

[1.]McKay Orthopaedic Research Laboratory, Department of Orthopaedic Surgery, University of Pennsylvania, Philadelphia, PA [2.]Department of Aerospace and Mechanical Engineering, University of Notre Dame, Notre Dame, IN [3.]Department of Bioengineering, University of Pennsylvania, Philadelphia, PA [4.]Trinity Centre for Biomedical Engineering, Trinity College Dublin, Dublin, Ireland

Abstract

Chondrocyte maturation during cartilage development occurs under diverse and dynamic mechanical environments. Mechanical stimulation through bioreactor culture may mimic these conditions to direct cartilage tissue engineering *in vitro*. Mechanical cues can promote chondrocyte homeostasis or hypertrophy and mineralization, depending potentially on the timing of load application. Here, we tested the effects of chondrogenic priming duration on the response of engineered human cartilage constructs to dynamic mechanical compression. We cultured human bone marrow stromal cells (hMSCs) in fibrin hydrogels under chondrogenic priming conditions for periods of 0, 2, 4, or 6 weeks prior to two weeks of either static culture or dynamic compression. We measured construct mechanical properties, cartilage matrix composition, and gene expression. Dynamic compression increased the equilibrium and dynamic modulus of the engineered tissue, depending on the duration of chondrogenic priming. For priming times of 2 weeks or greater, dynamic compression enhanced COL2A1 and AGGRECAN mRNA expression at the end of the loading period, but did not alter total collagen or glycosaminoglycan matrix deposition. Load initiation at priming times of 4 weeks or less repressed transient osteogenic signaling (RUNX2, OPN) and expression of CYR61, a YAP/TAZ-TEAD-target gene. No suppression of osteogenic gene expression was observed if loading was initiated after 6 weeks of in vitro priming, when mechanical stimulation was observed to increase the expression of type X collagen. Taken together, these data demonstrate that the duration of *in vitro* chondrogenic priming regulates the cell response to dynamic mechanical compression and suggests that early

[*]co-first authors

[†]co-senior authors

Author contributions

D.J.K. and J.D.B. conceived and supervised the research. A.M.M., D.J.K., and J.D.B. designed the experiments. A.M.M., E.A.E., D.J.K., and J.D.B. analyzed the data, and wrote the paper. All authors commented on and approved the final manuscript.

Conflicts of Interest

The authors have no conflicts of interest to disclose.

loading may preserve chondrocyte homeostasis while delayed loading may support cartilage maturation.

Introduction

Cartilage development initiates through condensation of mesenchymal progenitor cells and progresses by chondrogenic differentiation, maturation, and matrix production (Lefebvre and Bhattaram, 2010). When injured or diseased, cartilage has limited capacity for repair, creating a need for tissue-engineered solutions (Bian, 2013; Centola, 2013; Solorio, 2012; Dikina, 2017). In recent years, engineered cartilage tissues have also been used as *in vitro* models of osteoarthritis (Occhetta et al., 2019) and as cartilage templates for endochondral bone regeneration (Alsberg et al., 2002; Matsiko et al., 2018; McDermott et al., 2019; Occhetta et al., 2018; Sheehy et al., 2019; Thompson et al., 2016, 2015). These diverse applications all begin with *in vitro* engineering of human cartilage tissue, but the goals diverge as the tissues mature. For example, strategies for articular joint reconstruction prioritize maintenance of chondrocyte homeostasis, while disease models and engineered endochondral templates may prioritize *in vitro* progression through maturation, hypertrophy, and mineralization.

Cartilage development, maturation, and disease are regulated by mechanical cues. Mechanical forces exerted *in utero* direct proper development of the articular joints and of the endochondral skeleton (Felsenthal and Zelzer, 2017; Hamburger and Waugh, 1940; Nowlan et al., 2010; Verbruggen et al., 2018). Exercise-induced mechanical loading can also promote cartilage homeostasis and suppress cartilage degeneration in patients with osteoarthritis (Ytterberg, 1994; Roos, 2005). Similarly, for endochondral bone repair, studies from Stephan Perren (Hente et al., 2004; Perren and Cordey, 1980), and others (Claes et al., 2012, 2009, 1998; Claes and Heigele, 1999; Duncan and Turner, 1995; Goodship et al., 1993; Klein et al., 2003), demonstrate that mechanical cues, induced by interfragmentary motion in the fracture gap, determine whether healing occurs through differentiation of a cartilage callus or direct intramembranous ossification. Together, these observations point to mechanical forces as important regulators of chondroprogenitor behavior and fate for cartilage tissue engineering.

The optimal mechanical conditions for *in vitro* cartilage tissue engineering likely depend on the desired outcome (e.g., homeostasis, maturation, or mineralization). However, the interaction between the chondrocyte differentiation/maturation state and the timing of mechanical load initiation is poorly understood. Therefore, the goal of this study was to examine the effect of chondrogenic priming duration on the cell and tissue response to dynamic compression of engineered human cartilage *in vitro*.

Here, we chondrogenically primed fibrin hydrogel-encapsulated human bone marrow stromal cells (MSCs) to various stages of chondrogenic maturation (0, 2, 4, or 6 weeks of chondrogenic priming) prior to applying dynamic compression for two additional weeks. We then evaluated the effects of dynamic loading on tissue mechanical properties, cellular gene expression, and matrix deposition. We found that dynamic loading induced tissue stiffening and cellular mechanotransduction in manner dependent on priming duration,

and suppressed mineral deposition at latter stages of differentiation, but not when loading was applied after the onset of mineralization. These data demonstrate that chondrocyte mechanotransduction in engineered cartilage constructs depends on priming duration and suggest that early mechanical loading preserves chondrocyte homeostasis while delaying load permits hypertrophic progression. Thus, different mechanical loading conditions during engineered cartilage tissue culture may be preferred, depending on target application.

Materials and Methods

Study design

The goal of this study was to determine how the extent of chondrocyte maturation influences the mechanotransductive and chondrogenic response of hydrogel-embedded hMSCs to dynamic mechanical loading. We used a custom-made bioreactor to apply dynamic, unconfined compression to hMSC-laden hydrogels (Fig. 1A,B), which were then cultured under free-swelling conditions for either 0, 2, 4, or 6 weeks prior to 2 weeks of dynamic compression (Fig. 1C). Dynamically loaded samples were compared to time-matched free-swelling (FS) controls. Constructs were cultured in chondrogenic media throughout the study. The hydrogels were collected at the end of their loading cycle for analysis, as described below.

Cell culture

Human bone marrow stromal cells (hMSCs, P3) (Lonza) were expanded in high glucose Dulbecco's Modified Eagle's Medium (4.5 mg/mL glucose, 200 mM l-glutamine, hgDMEM), supplemented with 10% fetal bovine serum (FBS), 1% Penstrep, and 5 ng/mL FGF-2. The cultures were expanded to passage 3 (P3) and maintained in a humidified environment at 37°C, 5% CO2, and 5% O2.

Fibrin gel preparation and chondrogenic culture

Cells were then polymerized into fibrin hydrogels at 15×10^6 cells/mL. At 80% confluency, P3 hMSCs were trypsinized and resuspended in a 10,000 KIU/mL aprotinin solution (Nordic Pharma) with 19 mg/mL sodium chloride and 100mg/mL bovine fibrinogen (Sigma-Aldrich). Fibrinogen was polymerized into fibrin by combining cell suspensions 1:1 with a solution of 5 U/mL thrombin and 40 mM CaCl2 for a final solution of 50 mg/mL fibrinogen, 2.5 U/mL thrombin, 5000 KIU/mL aprotinin, 17 mg/mL sodium chloride, 20 mM CaCl2, and 15×10^6 cells/mL. The cell-laded hydrogel solution was then pipetted into 5 mm diameter × 2 mm thickness cylindrical agarose molds to create uniform constructs containing approximately 589,000 cells each.

Throughout the study, culture was maintained in chondrogenic media consisting of hgDMEM supplemented with 1% Penstrep, 100 KIU/mL aprotinin, 100 μg/mL sodium pyruvate, 40 μg/mL L -proline, 1.5 mg/mL bovine serum albumin, 4.7 μg/mL linoleic acid, 1x insulin-transferrin-selenium, 50 μg/mL L -ascorbic acid-2-phosphate, 100 nM dexamethasone (all Sigma-aldrich), and 10 ng/mL TGF-β3 (ProSpec-Tany TechnoGene Ltd., Israel). Fresh media was supplied every 3 days and culture was maintained in a humidified environment at 37°C, 5% CO2, and 5% O2.

Dynamic compression

Dynamic unconfined compressive loading was applied to the constructs using a custom-made bioreactor (Fig. 1B). Samples were loaded under sinusoidal displacement control, applied 2 hours per day, 5 days per week at 1 Hz to an amplitude of 10% strain, after a 0.01 N preload was applied. Control was programmed using an in-house MATLAB code.

Biochemical analysis

All constructs were harvested and analyzed at the end of their final loading cycle for DNA, sulfated glycosaminoglycan (sGAG) and collagen content (N = 5/group). Samples were digested overnight at 60°C in a solution of 125 μg/mL papain, 0.1 M sodium acetate, 5 mM L -cysteine, 0.05 M EDTA (all Sigma-Aldrich). DNA content was quantified with Hoechst Bisbenzimide 33258 dye assay (Sigma-Aldrich) as described previously (Kim et al., 1988), and sulfated glycosaminoglycan content was quantified using the dimethylmethylene blue dye-binding assay (Blyscan; Biocolor Ltd.). Collagen content was quantified by measurement of orthohydroxyproline using the dimethylaminobenzaldehyde and chloramine T assay (Kafienah and Sims, 2004). A hydroxyproline to collagen ratio of 1:7.69 was used (Ignat'eva et al., 2007) to infer total collagen content.

RNA isolation and qPCR

Total mRNA was extracted from fibrin/hMSC constructs after the final loading cycle using RNeasy mini kit (Qiagen). RNA (300ng) was reverse transcribed using into cDNA using High Capacity cDNA Reverse Transcription Kit (Applied Biosystems). Gene expression changes relative to free-swelling controls were quantified via real-time reverse transcription-polymerase chain reaction (qRT-PCR). Reactions were carried out in triplicate 20 μL volumes of 10 μL Sybr Green Master Mix (Applied Biosystems), 30 ng cDNA, 400 nM Sigma Kicqstart forward and reverse primers, on an ABI 7500 real-time PCR system (Applied Biosystems) with a profile of 95 °C for 10 min, and 40 cycles of denaturation at 95 °C for 15 sec, and annealing/amplification at 60 °C for 1 min. Quantification of target genes (Table 2) was determined against housekeeping reference gene GAPDH as fold change over free-swelling controls using the delta-delta Ct method (Schmittgen and Livak, 2008).

Histology and immunohistochemistry

Hydrogels were fixed in 4% paraformaldehyde (n = 2) overnight at 4°C. Constructs were halved and paraffin embedded cut surface down and sectioned at 5 μm to provide a cross-section of the hydrogel center. Sections were cleared in xylene, rehydrated in graded alcohols, and stained for sGAG in 1% Alcian blue with 0.1% Nuclear Fast Red counter stain.

Collagen deposition was identified through immunohistochemistry (Santa Cruz). Antigen retrieval was enzyme mediated (chondroitinase ABC, Sigma-Aldrich). Slides were blocked with Innovex Background Buster and incubated with primary antibody, diluted in PBS, overnight at 4°C. Slides were washed with PBS and incubated for 10 mins with universal rabbit IgG secondary antibody, followed by 10 mins with HRP enzyme, and DAB substrate for 5 mins (all Innovex). Sections were counterstained in Hematoxylin (VWR) and mounted

with Cytoseal XYL. Observations are qualitative only due to low sample sizes preventing histomorphometric quantitation of these outcomes.

Mechanical testing

Hydrogels were mechanically tested in unconfined compression (Zwick Roell Z005, Herefordshire, UK) between two steel platens and a 5N load cell. Hydrogels were hydrated in a PBS bath at room temperature. Equilibrium modulus was obtained via a stress relaxation test where a 10% strain was applied and maintained until equilibrium was reached. Dynamic modulus was determined after 10% strain was applied for 10 cycles at 1Hz and at 0.1Hz. In both tests a preload of 0.01N was applied to ensure contact between the hydrogel and machine platens.

Statistics

Statistical analyses were performed using either one- or two-way analysis of variance (ANOVA), as appropriate. Multiple comparisons between groups for one-way ANOVA were assessed by Tukey's multiple comparison test and two-way by Sidak's multiple comparison test. When necessary, data were log-transformed to ensure normality and homoscedasticity before ANOVA. Normality of dependent variables and residuals was verified by D'Agostino-Pearson omnibus and Brown-Forsythe tests, respectively. Statistical significance was set at $\alpha = 0.05$.

Results

Mechanical properties

First, we sought to determine how construct mechanical properties are impacted by the duration of chondrogenic priming and dynamic mechanical loading. To this end, we performed mechanical testing in unconfined compression following completion of the final loading cycle for each group, in comparison to time-matched free-swelling controls (Fig. 2). Both equilibrium and dynamic modulus increased significantly with the duration of priming time, and dynamic loading significantly increased the equilibrium modulus under conditions of 4 weeks of priming and dynamic modulus after both 4 and 6 weeks of priming.

Biochemical content

To determine the means by which dynamic compression increased construct mechanical properties, we first quantified the cellular and extracellular matrix content of the constructs (Fig. 3). The cellular number, measured by DNA content, was increased with increasing chondrogenic priming time, but was not significantly altered by loading (Fig. 3A). Chondrogenic priming significantly increased glycosaminoglycan (sGAG) deposition and sGAG/DNA, but differences between loading and free-swelling groups at each time point were not statistically significant (Fig. 3B, D). Collagen deposition, measured by hydroxyproline content, increased with priming time but was not significantly affected by loading either total or on a per-cell basis (Fig. 3C, E). Histological analysis of alcian blue-stained tissue sections revealed largely uniform acidic polysaccharide (i.e., sGAG) distribution throughout the constructs regardless of loading (Fig. 4). Therefore, while dynamic compression modestly influenced ECM composition overall, these data suggest

that other causes are required to fully explain the load-induced changes in construct mechanical properties.

Next, to determine whether the duration of chondrogenic priming influenced transient mechanotransductive responses to dynamic compression, we evaluated load-induced messenger RNA expression of genes associated with chondrogenesis, hypertrophy, and osteogenesis, immediately after the final loading cycle in each group. We compared loaded vs. free-swelling controls at each priming time point.

Chondrogenic gene expression

To evaluate chondrogenic gene expression, we quantified SOX9, aggrecan (ACAN), and collagen 2a1 (COL2A1) mRNA (Fig. 5). When loading was initiated immediately (no chondrogenic priming), dynamic loading significantly suppressed SOX9 (Fig. 5A) and had no effect on aggrecan (ACAN) expression (Fig. 5B), but significantly increased COL2A1 expression (Fig. 5C). At priming times of two weeks or more, SOX9 expression was not significantly altered by loading, while both ACAN and COL2A1 expression was significantly increased by dynamic compression. Together, these data indicate a significant effect of duration of priming on mechanotransduction, particularly the response of non-committed hMSCs vs. chondrocytes.

To evaluate the effects of loading on chondrogenic matrix deposition, we performed immunohistochemistry (IHC) staining for Col2a1 protein (Fig. 5D). Here, the observations are qualitative only. In the 0 and 2 weeks priming groups, Col2a1 staining was minimal regardless of loading conditions but prominent Col2a1 staining was observed in the 4 and 6 weeks priming groups.

Hypertrophic gene expression

Next, to evaluate mechanoregulation of hypertrophic gene expression, we quantified collagen 10a1 (COL10A1) and vascular endothelial growth factor (VEGF) mRNA, which are expressed at high levels by hypertrophic chondrocytes (Fig. 6). Dynamic compression significantly increased COL10A1 expression when loading was initiated immediately (no chondrogenic priming) and after 6 weeks of priming (Fig. 6A). VEGF regulation was variable with significant upregulation or downregulation depending on priming time (Fig. 6B).

Next, we performed qualitative immunohistochemistry (IHC) staining for Col10a1 protein (Fig. 6C). Col10a1 staining was spatially heterogeneous but qualitative differences between loading conditions and priming times were not clear.

Osteogenic gene expression

Finally, to evaluate mechanoregulation of osteogenic gene expression, we quantified Runt-related transcription factor 2 (RUNX2) and osteopontin (OPN) mRNA, markers of early and late osteoblastogenesis, respectively. Mechanoregulation of osteogenesis is mediated by the mechanosensitive transcriptional regulator, YAP (Dupont et al., 2011; Kegelman et al., 2018). We therefore also measured mRNA expression of YAP and the YAP-target gene

(through co-activation of the TEAD transcription factors), Cysteine-rich angiogenic inducer 61 (CYR61) (Fig. 7) (Mason et al., 2019). Loading decreased expression of RUNX2 after 4 weeks of priming, and OPN after 2 and 4 weeks of priming, but the suppressive effect of loading disappeared after 6 weeks of priming (Fig. 7A,B). To determine whether this was associated with mechanoregulation of the osteogenic transcriptional regulator, YAP, we evaluated CYR61 as a readout of YAP-TEAD signaling. YAP mechanotransduction is regulated at the protein level, mediated by YAP subcellular localization to the cytosol or the nucleus. As expected, therefore, we found no differences in YAP mRNA expression; however, CYR61 expression was significantly suppressed by dynamic compression after 0, 2, and 4 weeks of chondrogenic priming, in a manner consistent with the induction of chondrogenic gene expression and suppression of osteogenic gene expression (Fig. 7C,D).

To evaluate the functional effects of loading on mineral deposition, we performed alizarin red staining (Fig. 7C). Alizarin red staining was negative in all groups until 4 weeks priming, at which time limited positive staining was observed in free-swelling controls but not in those exposed to dynamic compression. After 6 weeks priming, both free-swelling and dynamic compression conditions exhibited modest alizarin red staining, comparable to free-swelling controls after 4 weeks of priming.

Discussion

In this study, we evaluated the effects of chondrogenic priming duration on the response of engineered human cartilage constructs to dynamic mechanical compression. We found that increased priming time significantly increased GAG and collagen deposition, increased construct mechanical properties, and qualitatively increased collagen II protein deposition. These observations demonstrate chondrogenic maturation with increased priming time. The response to dynamic loading depended on the extent of chondrogenic maturation in several ways. First, dynamic loading induced engineered construct stiffening, in both elastic and viscoelastic behavior, in a manner dependent on the duration of chondrogenic priming prior to load initiation. Further, dynamic loading induced priming time-dependent cellular mechanotransduction and transient expression of extracellular matrix genes, measured by gene expression immediately after the final loading bout. However, the amount and composition of the cartilaginous extracellular matrix depended only on the duration of chondrogenic culture and was not altered by mechanical loading at any time point. Taken together, these observations suggest several hypotheses for future study that may explain how loading increased mechanical properties without changes in bulk matrix amount or composition.

Cartilage mechanical properties are determined by the matrix organization and distribution as well as amount and composition. Thus, we speculate that mechanical load-induced changes in cartilage matrix organization or spatial distribution could contribute to altered mechanical properties. Previous studies on the mechanoresponsiveness of chondrogenically-primed MSCs or primary chondrocytes are consistent with our findings that dynamic loading enhances the mechanical properties of engineered cartilage. For example, studies from Mauck and colleagues, using dynamic loading applied continuously over 9–10 weeks of chondrogenic culture, found that loading increased engineered cartilage mechanical

properties by both promoting both type II collagen and GAG deposition (Mauck et al., 2002) and by altering its spatial distribution (Bian et al., 2010). In this study, we evaluated matrix deposition after two weeks of loading for different priming times prior to load initiation. Together with our observation that loading transiently increased ECM-regulated gene expression, this suggests that the two-week loading duration may be insufficient to observe substantial changes in matrix composition. However, this load duration was sufficient to alter mechanical properties. We and others have also adopted delayed loading regimes (Bian et al., 2012; Huang et al., 2010; Luo et al., 2015; Thorpe et al., 2010) to assess the response of established engineered cartilage to dynamic compression. Similar to the present data, these studies similarly observed increased mechanical properties after delayed loading (Huang et al., 2010; Luo et al., 2015), attributing it mainly to matrix organization (Luo et al., 2015; Thorpe et al., 2010) or matrix maturation and stress distribution (Huang et al., 2010). Here, we observed qualitative spatial heterogeneity in Col2a1 and Col10a1 protein deposition. These observations are consistent with our prior findings, which suggest that load-induced nutrient transport and/or ECM protein release into the culture bath may contribute to these spatial heterogeneities (Luo et al., 2015; Thorpe et al., 2010). Huang et al. observed no effect of loading on average matrix content, but using Fourier-transform infrared spectroscopy (FTIR) found that loading altered the spatial distribution of collagen deposition (Huang et al., 2010). Thus, we found that mechanical loading altered construct mechanical properties, in a manner dependent on the duration of chondrogenic priming, but future studies will be necessary to quantitatively define the effects of loading and priming time on matrix spatial heterogeneity.

Cartilage is a tissue of high cell density, and the mechanical properties of the cells themselves may also contribute to overall tissue mechanical properties. Here, we observed loading dependent changes in expression of Cyr61, a target gene for the mechanosensitive transcriptional regulators, YAP and TAZ. Recently, we discovered a mechanotransductive feedback loop, mediated by YAP and TAZ, that regulates the mechanical properties of the cell itself by modulating cytoskeletal maturation (Mason et al., 2019). To maintain cytoskeletal equilibrium, mechano-activated YAP and TAZ drive a transcriptional program that exerts negative feedback on myosin phosphorylation, modulating cytoskeletal tension, and suppression of YAP/TAZ expression or activity increases cell mechanical properties. In this study, we observed that increasing chondrogenic differentiation had no effect on YAP expression, but decreased YAP activity, with further YAP suppression by mechanical loading. This is consistent with our prior findings (McDermott et al., 2019) and with the current literature on the negative role of YAP in chondrocytes *in vitro* (Karystinou et al., 2015; Vanyai et al., 2020). Thus, we speculate that with increased chondrogenic maturation, load-induced suppression of YAP transcriptional activity (measured here by the YAP/TAZ-TEAD target gene, Cyr61) may play a role in the maintenance of a chondrogenic phenotype. With extended maturation (6 weeks of chondrogenic priming), loading no longer suppressed YAP activity, allowing maturation in the presence of loading.

Consistent with these changes in mechanotransductive gene expression, we also found that dynamic loading regulated expression of chondrogenic mRNAs. Mechanical load-induced mRNA expression is transient (McDermott et al., 2019) and PCR analysis provides a snap-shot of mRNA abundance at the time of assay. As these experiments were designed

to vary priming time, but not loading duration, qPCR reactions and gene expression comparisons were performed only between loaded and non-loaded conditions at each time point, and cannot be compared over time. Thus, while load-induced gene expression exhibited variability, we are unable to assess gene expression trends as a function of tissue maturation. With no priming, dynamic loading upregulated genes commonly associated with hypertrophy (Col10a1, VEGF) compared to static controls. It should be noted that expression of such canonical hypertrophic markers can also increase during the early stages of chondrogenesis (Mwale et al., 2006) so care must be taken when interpreting changes in the expression of genes such as Col10a1 in the early stages of chondrogenesis. Immediate loading also induced mismatched chondrogenic gene expression (downregulation of Sox9, and upregulation of Col2a1), consistent with similar studies (Steinmetz and Bryant, 2011). We observed modest upregulation of VEGF with immediate loading, whereas our previous data shows no change compared to free swelling controls (McDermott et al., 2019). We also observed downregulation of SOX9, coupled with an upregulation of COL2 expression, in contrast to similar studies that observed co-regulation of COL2, ACAN and SOX9 (McDermott et al., 2019; Michalopoulos et al., 2012; Terraciano et al., 2007). A possible explanation is the relative transience of SOX9 message expression compared to matrix genes like ACAN and COL2. As demonstrated by Cote et al., instantaneous gene expression, even at the single-cell level, does not predict cartilage matrix deposition, which rather reflects accumulation at the evaluated timepoint (Cote et al., 2016). While our experimental design did not allow us to compare gene expression levels over time or with matrix deposition, these data demonstrate mechanotransductive gene expression responses to dynamic loading, dependent on the duration of priming time.

Taken together, we provide new evidence that dynamic mechanical compression influences engineered cartilage tissue formation in a manner dependent on the chondrogenic maturation state at the time of load initiation. Future research is warranted to dissect the cellular and molecular mechanisms by which chondrocytes receive and interpret mechanical cues and the functional consequences on cartilage maintenance or maturation for tissue engineering applications.

Limitations

The goal of this study was to observe the effects of chondrogenic priming of human MSCs under dynamic compression, but the study has several limitations that influence our interpretation. First, although MSCs are of potential translational interest for tissue engineering, they may not reflect the biology of the limb bud progenitor cells that give rise to the cartilage anlage in development (Kegelman et al., 2018) or of the periosteal progenitor cells that give rise to the fracture callus (Kegelman et al., 2020). Second, MSCs exhibit extensive donor-donor variability. In this study, we used commercially-sourced MSCs from pooled donors, and this study was not designed to dissect the contributions of donor variability to the observed responses. Third, both gene expression and mechanical testing analyses were performed on bulk tissues, which may mask spatial heterogeneity of cellular mechanotransduction, matrix-associated gene expression, and local mechanical properties. Fourth, this study used only a two-week loading duration. Both shorter and longer durations of mechanical loading would enable dissection of the effects of load timing

on acute mechanotransduction and tissue production, respectively. Fifth, as the assays used cannot be performed longitudinally, we did not assess the chondrogenic maturation state of the same samples both prior to and after loading. However, we designed the experiment such that free-swelling controls were evaluated both at the time points of load initiation and at termination of loading. Free-swelling controls were assayed at 0, 2, 4, and 6 weeks, corresponding to the load initiation time points at 0, 2, 4, and 6 weeks. These may be compared for objective assays including Collagen, GAG, and DNA quantification, as well as histology and immunostaining to infer the chondrogenic maturation state at the time points of load initiation. Finally, while our observations of the effects of loading on spatial heterogeneity in matrix deposition are consistent with prior reports from both our own and other groups, low sample sizes precluded histomorphometric quantitation of these outcomes.

Acknowledgements

This work was supported by the Naughton Foundation (to A.M.M.), the NIH's National Institute of Arthritis and Musculoskeletal and Skin Diseases under award number R01AR074948 (to JDB), the Penn Center for Musculoskeletal Disorders under award number P30AR069619 (to JDB), and the Center for Engineering Mechanobiology (CEMB), an NSF Science and Technology Center, under grant agreement CMMI: 15-48571. The contents of this publication are solely the responsibility of the authors and do not necessarily represent the official views of the NIH, the National Science Foundation, or other funding agencies.

References

Alsberg E, Anderson KW, Albeiruti A, Rowley JA, Mooney DJ, 2002. Engineering growing tissues. Proc. Natl. Acad. Sci. U. S. A99, 12025–12030. [PubMed: 12218178]

Bian L, Fong JV, Lima EG, Stoker AM, Ateshian GA, Cook JL, Hung CT, 2010. Dynamic mechanical loading enhances functional properties of tissue-engineered cartilage using mature canine chondrocytes. Tissue Eng. - Part A16, 1781–1790. 10.1089/ten.tea.2009.0482 [PubMed: 20028219]

Bian L, Zhai DY, Zhang EC, Mauck RL, Burdick JA, 2012. Dynamic compressive loading enhances cartilage matrix synthesis and distribution and suppresses hypertrophy in hMSC-laden hyaluronic acid hydrogels. Tissue Eng. Part A18, 715–24. 10.1089/ten.TEA.2011.0455 [PubMed: 21988555]

Claes L, Recknagel S, Ignatius A, 2012. Fracture healing under healthy and inflammatory conditions. Nat. Rev. Rheumatol8, 133–43. 10.1038/nrrheum.2012.1 [PubMed: 22293759]

Claes L, Veeser A, Göckelmann M, Simon U, Ignatius A, 2009. A novel model to study metaphyseal bone healing under defined biomechanical conditions. Arch. Orthop. Trauma Surg129, 923–928. 10.1007/s00402-008-0692-9 [PubMed: 18654792]

Claes LE, Heigele CA, 1999. Magnitudes of local stress and strain along bony surfaces predict the course and type of fracture healing. J. Biomech32, 255–266. 10.1016/S0021-9290(98)00153-5 [PubMed: 10093025]

Claes LE, Heigele CA, Neidlinger-Wilke C, Kaspar D, Seidl W, Margevicius KJ, Augat P, 1998. Effects of mechanical factors on the fracture healing process. Clin. Orthop. Relat. Res10.1097/00003086-199810001-00015

Cote AJ, McLeod CM, Farrell MJ, McClanahan PD, Dunagin MC, Raj A, Mauck RL, 2016. Single-cell differences in matrix gene expression do not predict matrix deposition. Nat. Commun7. 10.1038/ncomms10865

Duncan RL, Turner CH, 1995. Mechanotransduction and the Functional Response of Bone to Mechanical Strain R. Calcif. Tissue Int57, 344–358. [PubMed: 8564797]

Dupont S, Morsut L, Aragona M, Enzo E, Giulitti S, Cordenonsi M, Zanconato F, Le Digabel J, Forcato M, Bicciato S, Elvassore N, Piccolo S, 2011. Role of YAP/TAZ in mechanotransduction. Nature474, 179–83. 10.1038/nature10137 [PubMed: 21654799]

Felsenthal N, Zelzer E, 2017. Mechanical regulation of musculoskeletal system development. Development144, 4271–4283. 10.1242/dev.151266 [PubMed: 29183940]

Goodship AE, Watkins PE, Rigby HS, Kenwright J, 1993. The role of fixator frame stiffness in the control of fracture healing. An experimental study. J. Biomech26, 1027–1035. 10.1016/S0021-9290(05)80002-8 [PubMed: 8408085]

Hamburger V, Waugh M, 1940. The Primary Development of the Skeleton in Nerveless and Poorly Innervated Limb Transplants of Chick Embryos. Physiol. Zool13, 367–382.

Hente R, Füchtmeier B, Schlegel U, Ernstberger a, Perren SM, 2004. The influence of cyclic compression and distraction on the healing of experimental tibial fractures. J. Orthop. Res22, 709–15. 10.1016/j.orthres.2003.11.007 [PubMed: 15183425]

Huang AH, Farrell MJ, Kim M, Mauck RL, 2010. LONG-TERM DYNAMIC LOADING IMPROVES THE MECHANICAL PROPERTIES OF CHONDROGENIC MESENCHYMAL STEM CELL-LADEN HYDROGELS. Eur. Cells Mater19, 72–85. 10.22203/ecm.v019a08

Ignat'eva NY, Danilov NA, Averkiev SV, Obrezkova MV, Lunin VV, Sobol' EN, 2007. Determination of hydroxyproline in tissues and the evaluation of the collagen content of the tissues. J. Anal. Chem62, 51–57. 10.1134/S106193480701011X

Kafienah W, Sims TJ, 2004. Biochemical methods for the analysis of tissue-engineered cartilage. Methods Mol. Biol238, 217–230. 10.1385/1-59259-428-x:217 [PubMed: 14970450]

Karystinou A, Roelofs AJ, Neve A, Cantatore FP, Wackerhage H, De Bari C, 2015. Yes-associated protein (YAP) is a negative regulator of chondrogenesis in mesenchymal stem cells. Arthritis Res. Ther17, 1–14. 10.1186/s13075-015-0639-9 [PubMed: 25566937]

Kegelman CD, Mason DE, Dawahare JH, Horan DJ, Vigil GD, Howard SS, Robling AG, Bellido TM, Boerckel JD, 2018. Skeletal cell YAP and TAZ combinatorially promote bone development. FASEB Jfj.201700872R. 10.1096/fj.201700872R

Kegelman CD, Nijsure MP, Moharrer Y, Pearson HB, Dawahare JH, Jordan KM, Qin L, Boerckel JD, 2020. YAP and TAZ Promote Periosteal Osteoblast Precursor Expansion and Differentiation for Fracture Repair. J. Bone Miner. Res10.1002/jbmr.4166

Kim YJ, Sah RLY, Doong JYH, Grodzinsky AJ, 1988. Fluorometric assay of DNA in cartilage explants using Hoechst 33258. Anal. Biochem174, 168–176. 10.1016/0003-2697(88)90532-5 [PubMed: 2464289]

Klein P, Schell H, Streitparth F, Heller M, Kassi JP, Kandziora F, Bragulla H, Haas NP, Duda GN, 2003. The initial phase of fracture healing is specifically sensitive to mechanical conditions. J. Orthop. Res21, 662–669. 10.1016/S0736-0266(02)00259-0 [PubMed: 12798066]

Lefebvre V, Bhattaram P, 2010. Vertebrate skeletogenesis. Curr. Top. Dev. Biol90, 291–317. 10.1016/S0070-2153(10)90008-2 [PubMed: 20691853]

Luo L, Thorpe SD, Buckley CT, Kelly DJ, 2015. The effects of dynamic compression on the development of cartilage grafts engineered using bone marrow and infrapatellar fat pad derived stem cells. Biomed. Mater10. 10.1088/1748-6041/10/5/055011

Mason DE, Collins JM, Dawahare JH, Nguyen TD, Lin Y, Voytik-Harbin SL, Zorlutuna P, Yoder MC, Boerckel JD, 2019. YAP and TAZ limit cytoskeletal and focal adhesion maturation to enable persistent cell motility. J. Cell Biol218, 1369–1389. 10.1083/jcb.201806065 [PubMed: 30737263]

Matsiko A, Thompson EM, Lloyd-Griffith C, Cunniffe GM, Vinardell T, Gleeson JP, Kelly DJ, O'Brien FJ, 2018. An endochondral ossification approach to early stage bone repair: Use of tissue-engineered hypertrophic cartilage constructs as primordial templates for weight-bearing bone repair. J. Tissue Eng. Regen. Med12, e2147–e2150. 10.1002/term.2638 [PubMed: 29327428]

Mauck RL, Seyhan SL, Ateshian GA, Hung CT, 2002. Influence of seeding density and dynamic deformational loading on the developing structure/function relationships of chondrocyte-seeded agarose hydrogels. Ann. Biomed. Eng30, 1046–1056. 10.1114/1.1512676 [PubMed: 12449765]

McDermott AM, Herberg S, Mason DE, Collins JM, Pearson HB, Dawahare JH, Tang R, Patwa AN, Grinstaff MW, Kelly DJ, Alsberg E, Boerckel JD, 2019. Recapitulating bone development through engineered mesenchymal condensations and mechanical cues for tissue regeneration. Sci. Transl. Med11, eaav7756. 10.1126/scitranslmed.aav7756 [PubMed: 31167930]

Michalopoulos E, Knight RL, Korossis S, Kearney JN, Fisher J, Ingham E, 2012. Development of methods for studying the differentiation of human mesenchymal stem cells under cyclic compressive strain. Tissue Eng. - Part C Methods18, 252–262. 10.1089/ten.tec.2011.0347 [PubMed: 22047076]

Mwale F, Stachura D, Roughley P, Antoniou J, 2006. Limitations of using aggrecan and type X collagen as markers of chondrogenesis in mesenchymal stem cell differentiation. J. Orthop. Res24, 1791–1798. 10.1002/jor.20200 [PubMed: 16779832]

Nowlan NC, Sharpe J, Roddy KA, Prendergast PJ, Murphy P, 2010. Mechanobiology of embryonic skeletal development: Insights from animal models. Birth Defects Res. Part C Embryo Today Rev90, 203–213. 10.1002/bdrc.20184

Occhetta P, Mainardi A, Votta E, Vallmajo-Martin Q, Ehrbar M, Martin I, Barbero A, Rasponi M, 2019. Hyperphysiological compression of articular cartilage induces an osteoarthritic phenotype in a cartilage-on-a-chip model. Nat. Biomed. Eng3, 545–557. 10.1038/s41551-019-0406-3 [PubMed: 31160722]

Occhetta P, Pigeot S, Rasponi M, Dasen B, Mehrkens A, Ullrich T, Kramer I, Guth-Gundel S, Barbero A, Martin I, 2018. Developmentally inspired programming of adult human mesenchymal stromal cells toward stable chondrogenesis. Proc. Natl. Acad. Sci. U. S. A115, 4625–4630. 10.1073/pnas.1720658115 [PubMed: 29666250]

Perren SM, Cordey J, 1980. The concept of interfragmentary strain. Curr. concepts Intern. Fixat. Fract63–77.

Schmittgen TD, Livak KJ, 2008. Analyzing real-time PCR data by the comparative CT method. Nat. Protoc3, 1101–1108. 10.1038/nprot.2008.73 [PubMed: 18546601]

Sheehy EJ, Kelly DJ, O'Brien FJ, 2019. Biomaterial-based endochondral bone regeneration: a shift from traditional tissue engineering paradigms to developmentally inspired strategies. Mater. Today Bio3, 100009. 10.1016/j.mtbio.2019.100009

Steinmetz NJ, Bryant SJ, 2011. The effects of intermittent dynamic loading on chondrogenic and osteogenic differentiation of human marrow stromal cells encapsulated in RGD-modified poly(ethylene glycol) hydrogels. Acta Biomater. 7, 3829–3840. 10.1016/j.actbio.2011.06.031 [PubMed: 21742067]

Terraciano V, Hwang N, Moroni L, Park H. Bin, Zhang Z, Mizrahi J, Seliktar D, Elisseeff J, 2007. Differential Response of Adult and Embryonic Mesenchymal Progenitor Cells to Mechanical Compression in Hydrogels. Stem Cells25, 2730–2738. 10.1634/stemcells.2007-0228 [PubMed: 17702983]

Thompson EM, Matsiko A, Farrell E, Kelly DJ, O'Brien FJ, 2015. Recapitulating endochondral ossification: a promising route to in vivo bone regeneration. J. Tissue Eng. Regen. Med9, 889–902. 10.1002/term.1918 [PubMed: 24916192]

Thompson EM, Matsiko A, Kelly DJ, Gleeson JP, O'Brien FJ, 2016. An Endochondral Ossification-Based Approach to Bone Repair: Chondrogenically Primed Mesenchymal Stem Cell-Laden Scaffolds Support Greater Repair of Critical-Sized Cranial Defects Than Osteogenically Stimulated Constructs in Vivo. Tissue Eng. - Part A22, 556–567. 10.1089/ten.tea.2015.0457 [PubMed: 26896424]

Thorpe SD, Buckley CT, Vinardell T, O'Brien FJ, Campbell VA, Kelly DJ, 2010. The response of bone marrow-derived mesenchymal stem cells to dynamic compression following tgf-β3 induced chondrogenic differentiation. Ann. Biomed. Eng38, 2896–2909. 10.1007/s10439-010-0059-6 [PubMed: 20458627]

Vanyai HK, Prin F, Guillermin O, Marzook B, Boeing S, Howson A, Saunders RE, Snoeks T, Howell M, Mohun TJ, Thompson B, 2020. Control of skeletal morphogenesis by the Hippo-YAP/TAZ pathway. Development147. 10.1242/dev.187187

Verbruggen SW, Kainz B, Shelmerdine SC, Hajnal JV, Rutherford MA, Arthurs OJ, Phillips ATM, Nowlan NC, 2018. Stresses and strains on the human fetal skeleton during development. J. R. Soc. Interface15, 20170593. 10.1098/rsif.2017.0593 [PubMed: 29367236]

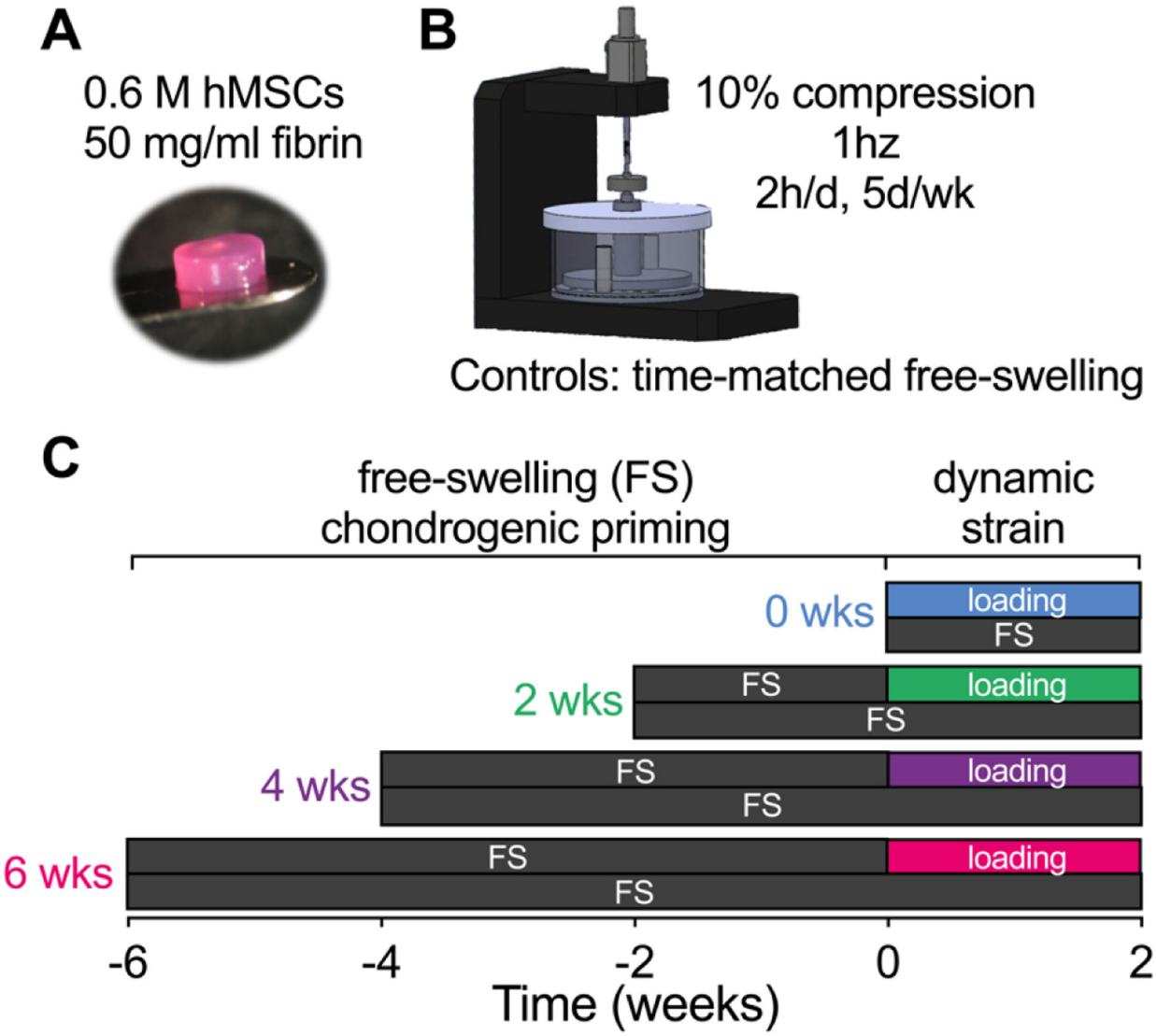

Figure 1: Bioreactor setup and loading timeline.

(A) hMSC-laden hydrogels (P3, 589,000 cells, 50mg/mL fibrinogen) were subjected to different degrees of chondrogenic priming (0wks, 2wks, 4wks, 6wks) followed by 2 weeks of (B) dynamic compression in a custom-made bioreactor. (C) All samples were collected after their loading cycle and compared to free-swelling controls at the same time.

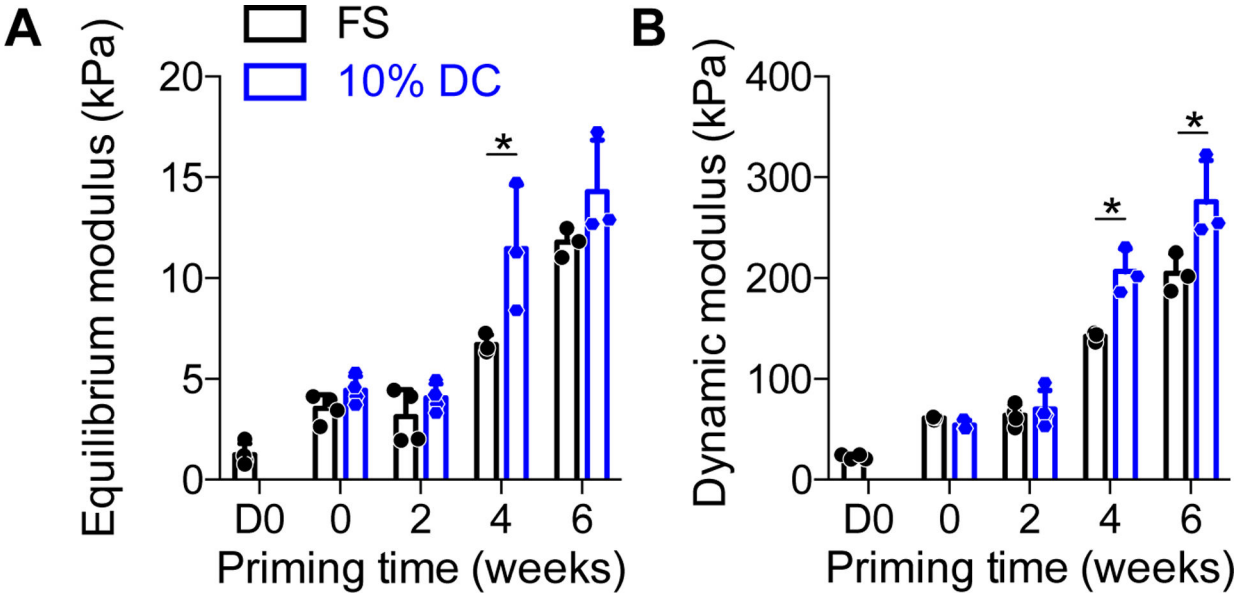

Figure 2: Mechanical properties of chondrogenically-primed hMSC constructs under free-swelling (FS) or 10% dynamic compression (DC) conditions.

Samples were tested in unconfined compression to determine equilibrium modulus, E´ (A) and dynamic modulus, E´´ (B) at the end of the final loading cycle for each group, in comparison to time-matched free-swelling controls. Data are shown as displayed as mean ± s.d. with individual data points. Differences between groups and time points were evaluated by two-way ANOVA followed by Sidak's multiple comparison test. The significance threshold was set at α=0.05. Both equilibrium and dynamic modulus increased significantly with time. Significant differences between free-swelling (FS) and dynamic compression (DC) groups are indicated with asterisks. N = 3 – 4 per group.

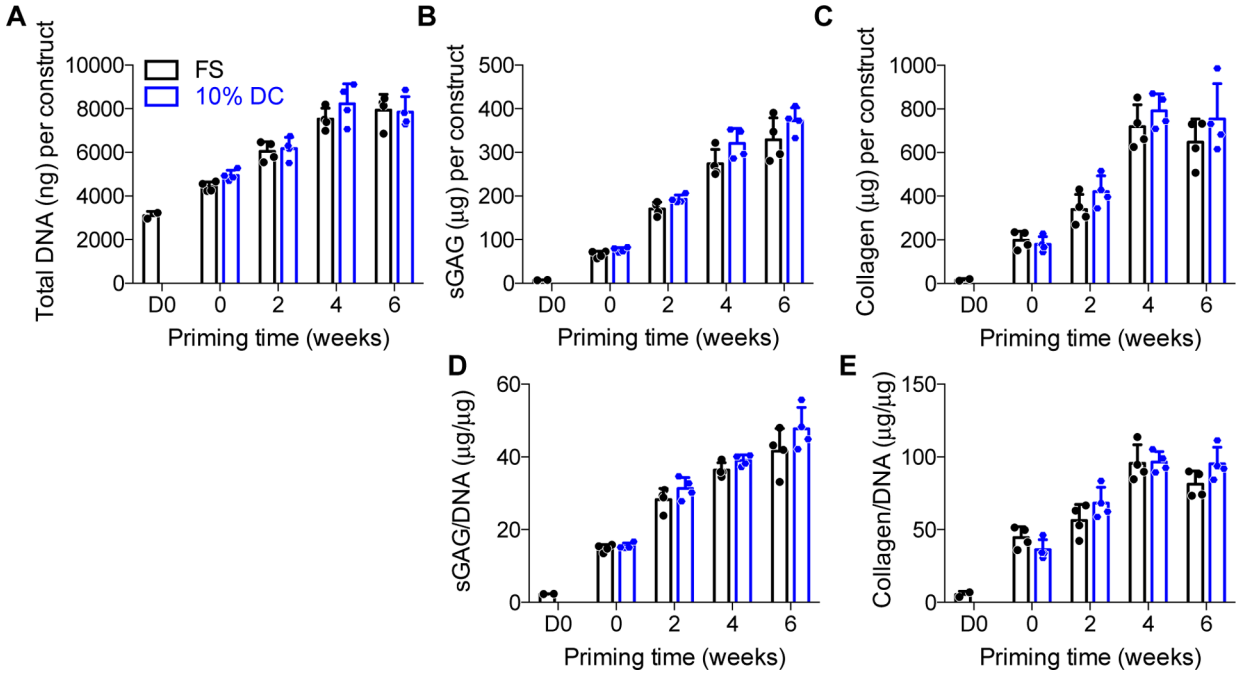

Figure 3: Biochemical content of chondrogenically-primed hMSC constructs under free-swelling (FS) or 10% dynamic compression (DC) conditions.

Samples were digested and assayed for biochemical content at the end of the final loading cycle for each group, in comparison to time-matched free-swelling controls. Each construct was assayed for total DNA content (A), total sulfated glycosaminoglycans (sGAG) (B), and total collagen (C). sGAG (D) and collagen (E) were then normalized, on a per-sample basis, to DNA content. Data are displayed as mean ± s.d. with individual data points. Differences between groups and time points were evaluated by two-way ANOVA followed by Sidak's multiple comparison test. The significance threshold was set at α=0.05. All measures increased significantly with time. ANOVA analysis indicated a significant effect of time for sGAG and sGAG/DNA, but there were no differences for individual comparisons between FS and DC at any time point. N = 3 – 4 per group.

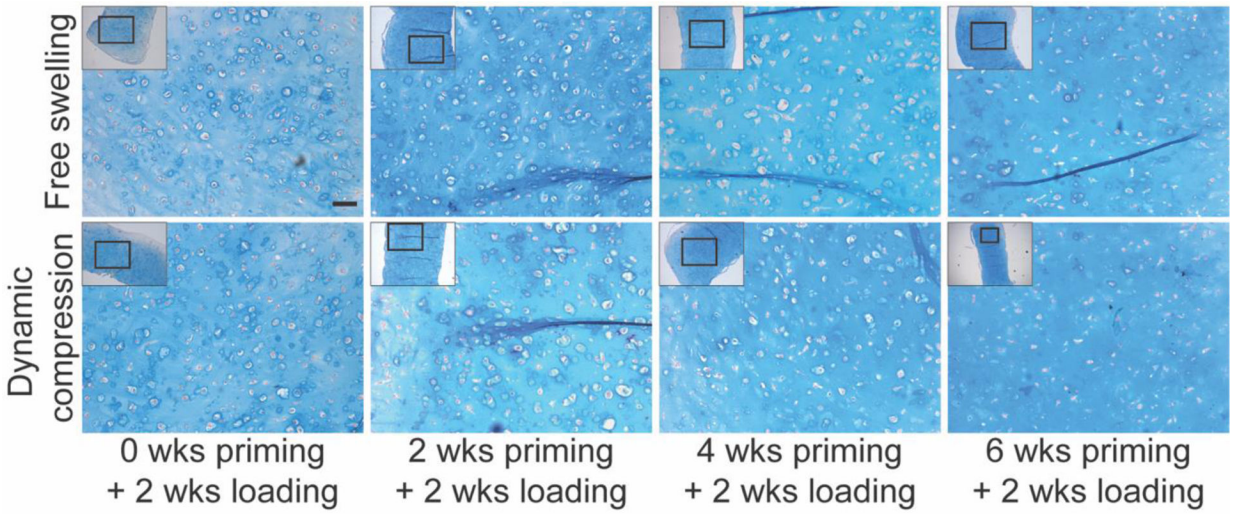

Figure 4: Alcian blue staining of glycosaminoglycans in chondrogenically-primed hMSC constructs under free-swelling (FS) or 10% dynamic compression (DC) conditions.

Samples were fixed and sectioned at the end of the final loading cycle for each group and stained with Alcian blue/Nuclear Fast Red. Scale bar = 100 μm.

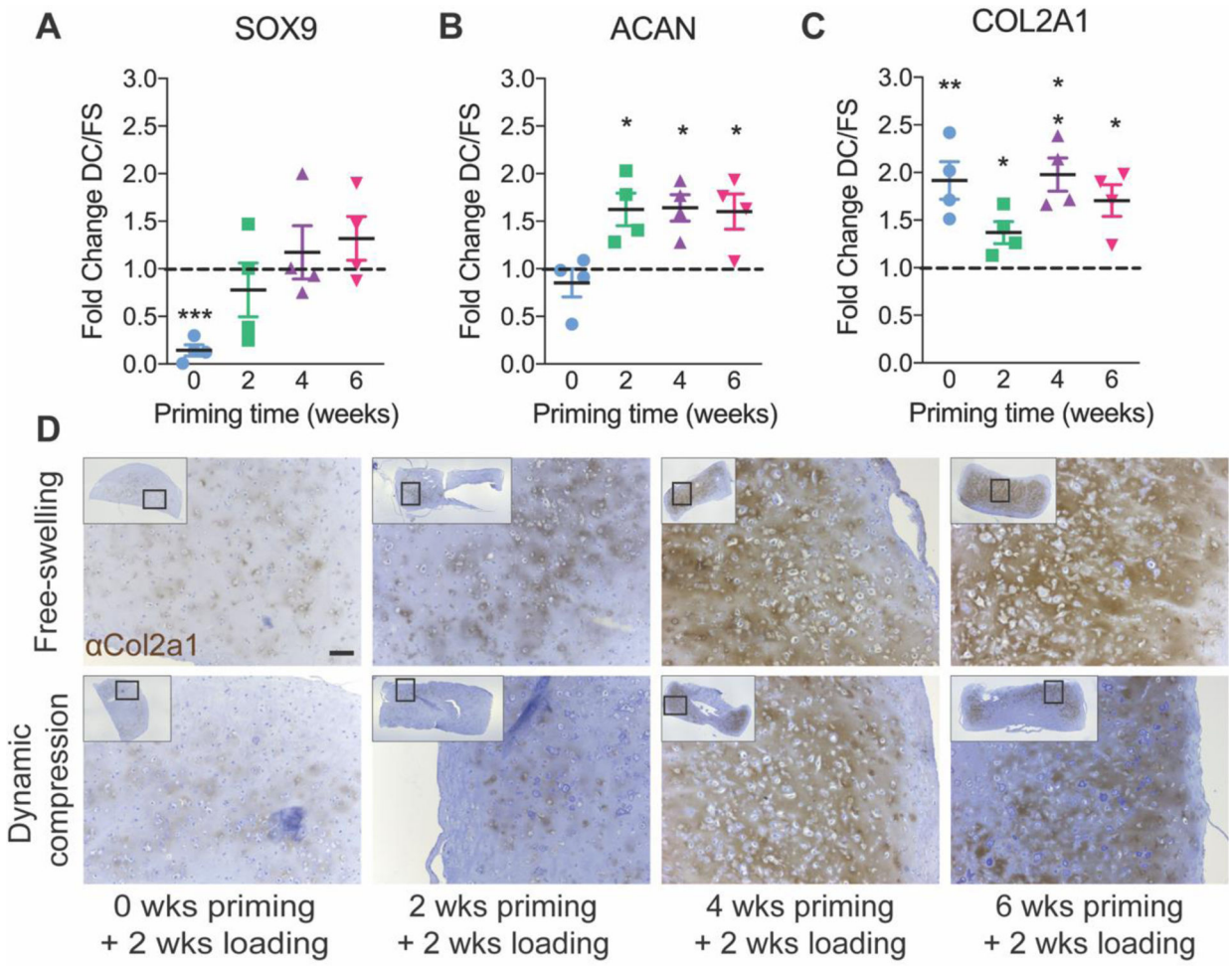

Figure 5: Chondrogenic gene expression and Col2a1 immunohistochemistry under free-swelling (FS) or 10% dynamic compression (DC) conditions.

Samples were analyzed immediately after the final loading cycle in each group for mRNA expression of SOX9 (A), ACAN (B), and COL2A1 (C), calculated as fold change over free-swelling controls, normalized to GAPDH. Data are shown as mean ± s.d. with individual data points. ANOVA with Tukey's post-hoc tests were used to determine significance (* $p < 0.05$, ** $p < 0.01$). Immunohistochemistry for Col2a1 (D) with hematoxylin counterstain (scale bar = 100 μm). N = 4 per group.

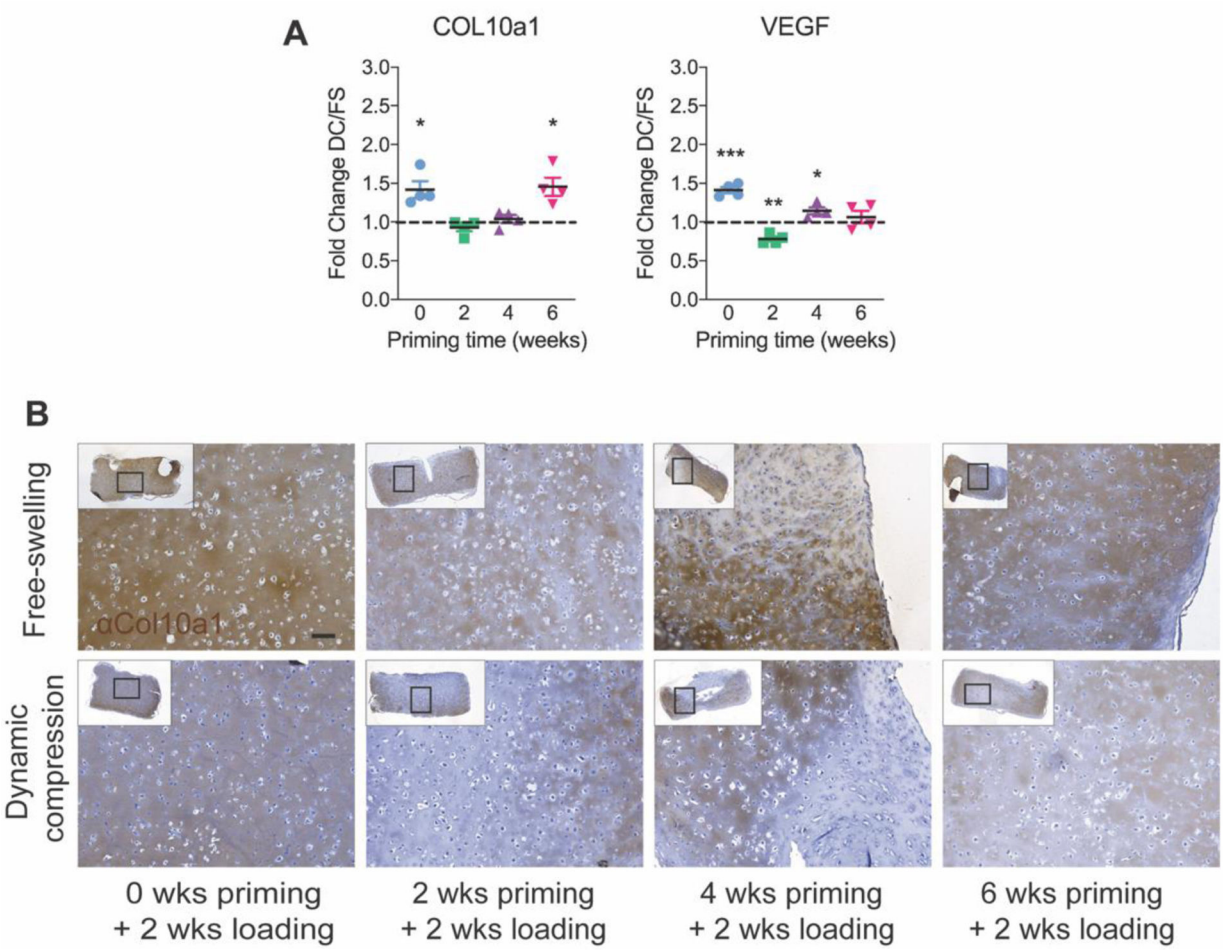

Figure 6: Hypertrophic gene expression and Col10a1 immunohistochemistry under free-swelling (FS) or 10% dynamic compression (DC) conditions.

Samples were analyzed immediately after the final loading cycle in each group for mRNA expression of COL10A1 (A) and VEGF (B), calculated as fold change over free-swelling controls, normalized to GAPDH. Data are shown as mean ± s.d. with individual data points. ANOVA with Tukey's post-hoc tests were used to determine significance (* $p < 0.05$, ** $p < 0.01$). Immunohistochemistry for Col10a1 (C) with hematoxylin counterstain (scale bar = 100 μm). N = 4 per group.

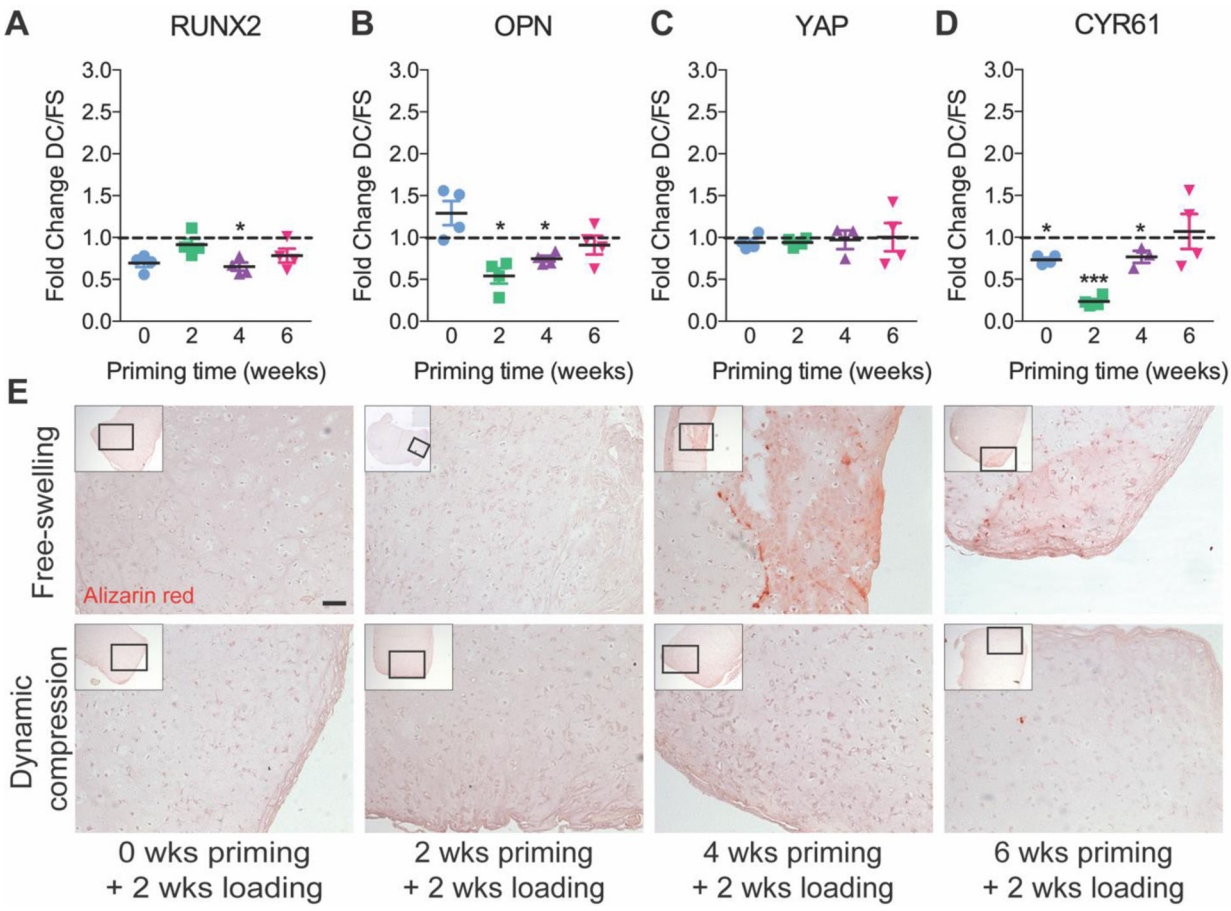

Figure 7: Osteogenic gene expression and mineral deposition under free-swelling (FS) or 10% dynamic compression (DC) conditions.

Samples were analyzed immediately after the final loading cycle in each group for mRNA expression of RUNX2 (A), osteopontin (OPN) (B), Yes-associated protein (YAP) (C), and the YAP-TEAD transcriptional target gene, Cysteine-rich angiogenic inducer 61 (CYR61) (D), calculated as fold change over free-swelling controls, normalized to GAPDH. Data are shown as mean ± s.d. with individual data points. ANOVA with Tukey's post-hoc tests were used to determine significance (* $p < 0.05$, ** $p < 0.01$). Mineral deposition was evaluated by alizarin red staining on histological sections (E) (scale bar = 100 μm). N = 4 per group.

Table 2 :

qPCR target genes

Gene	Sequence 5'−3'	Accession Number
GAPDH	Fwd CTTTTGCGTCGCCAG Rev TTGATGGCAACAATATCCAC	NM_002046
Sox9	Fwd CTCTGGAGACTTCTGAACG Rev AGATGTGCGTCTGCTC	NM_000346
ACAN	Fwd TGCGGGTCAACAGTGCCTATC Rev CACGATGCCTTTCACCACGAC	NM_001135
Col2a1	Fwd GAAGAGTGGAGACTACTGG Rev CAGATGTGTTTCTTCTCCTTG	NM_033150
OPN (SPP1)	Fwd GACCAAGGAAAACTCACTAC Rev CTGTTTAACTGGTATGGCAC	NM_001251829
RUNX2	Fwd AAGCTTGATGACTCTAAACC Rev TCTGTAATCTGACTCTGTCC	NM_001015051
Col10a1	Fwd GCTAGTATCCTTGAACTTGG Rev CCTTTACTCTTTATGGTGTAGG	NM_000493
VEGFA	Fwd AATGTGAATGCAGACCAAAG Rev GACTTATACCGGGATTTCTTG	NM_001204384